

## Research Article

# Monitoring of Rotor-Stator Interaction in Pump-Turbine Using Vibrations Measured with On-Board Sensors Rotating with Shaft

Cristian G. Rodriguez,<sup>1</sup> Borja Mateos-Prieto,<sup>2</sup> and Eduard Egusquiza<sup>2</sup>

<sup>1</sup> Department of Mechanical Engineering, University of Concepcion, Edmundo Larenas 270 Interior, 4070409 Concepcion, Chile

<sup>2</sup> Centre of Industrial Diagnostics and Fluid Dynamics (CDIF), Technical University of Catalonia (UPC), Av. Diagonal 647, 08028 Barcelona, Spain

Correspondence should be addressed to Cristian G. Rodriguez; [cristian.rodriguez@udec.cl](mailto:cristian.rodriguez@udec.cl)

Received 10 April 2013; Accepted 24 May 2013; Published 12 February 2014

Academic Editor: Valder Steffen

Copyright © 2014 Cristian G. Rodriguez et al. This is an open access article distributed under the Creative Commons Attribution License, which permits unrestricted use, distribution, and reproduction in any medium, provided the original work is properly cited.

Current trends in design of pump-turbines have led into higher rotor-stator interaction (RSI) loads over impeller-runner. These dynamic loads are of special interest having produced catastrophic failures in pump-turbines. Determining RSI characteristics facilitates the proposal of actions that will prevent these failures. Pressure measurements all around the perimeter of the impeller-runner are appropriate to monitor and detect RSI characteristics. Unfortunately most installed pump-turbines are not manufactured with in-built pressure sensors in appropriate positions to monitor RSI. For this reason, vibration measurements are the preferred method to monitor RSI in industry. Usually vibrations are measured in two perpendicular radial directions in bearings where valuable information could be lost due to bearing response. In this work, in order to avoid the effect of bearing response on measurement, two vibration sensors are installed rotating with the shaft. The RSI characteristics obtained with pressure measurements were compared to those determined using vibration measurements. The RSI characteristics obtained with pressure measurements were also determined using vibrations measured rotating with shaft. These RSI characteristics were not possible to be determined using the vibrations measured in guide bearing. Finally, it is recommended to measure vibrations rotating with shaft to detect RSI characteristics in installed pump-turbines as a more practical and reliable method to monitor RSI characteristics.

## 1. Introduction

Power in a pumped-storage hydropower station is proportional to flow-rate and net-head. In order to minimize the expenses of the civil construction, it is desirable to have smaller reservoirs and penstock. To have the highest possible flow-rate with smaller penstock it is necessary to have a high flow velocity. To have a high flow velocity it is necessary to have the highest possible net-head. When the net-head is increased, then the pressure in the impeller-runner is also increased. For these reasons the flow velocity and pressure in newer designs of pump-turbines are raised as much as possible in comparison to those found in older designs. This raise in the flow velocity and pressure leads to higher excitation fluid forces over the impeller-runner. One of the fluid forces over the impeller-runner that significantly

increases with higher flow velocity and pressure is due to the rotor-stator interaction (RSI). RSI is generated because pump-turbines consist of a bladed rotor (bladed impeller-runner) and a vaned stator (guide vanes or wicket gates in diffuser-distributor). When the pump-turbine is under operation, there is a fluid-dynamic load every time a blade passes in front of a guide vane, producing a periodic load at blade passing frequency and its harmonics [1–7]. Forces due to RSI are applied to the impeller-runner which is designed to be as small as possible in order to minimize manufacture and transport expenses leading to a reduced thickness/weight ratio and a high power/weight ratio. Because of electricity grid requirements, in order to adjust the power to instant demand the pump-turbine must be able to work at partial loads, needing a high level of regulation capacity. This is only affordable in a single stage impeller-runner. For all

these reasons, new designs of impeller-runners in pump-turbines support higher RSI excitation forces, have more flexible and smaller structures, and present higher pressure difference in a single stage. The current trends in the design lead to the generation of high vibration levels due to RSI; this could cause important damage as reported in Coutu et al. [8] and Egusquiza et al. [9]: Coutu et al. [8] showed that a 447 MW pump-turbine suffered major cracks on impeller-runner blades after just 200 hours of operation and Egusquiza et al. [9] showed a catastrophic failure where a part of crown detached from the impeller-runner while the machine was in operation in a 110 MW pump-turbine. These failures were produced by fatigue due to high level of dynamic stresses induced by RSI. The corrective actions to overcome these failures resulted in important out of schedule stoppages with the consequent loss in production. It is important to mention that these trends in design mainly affect the impeller-runner and do not affect significantly the rest of the machine (motor-generator, shaft, bearings, etc.), which have not changed significantly in the last years. In the latest designs of pump-turbines, RSI has become the most important excitation over the impeller-runner and usually produces the highest vibration levels measured in the whole pump-turbine [7]. In practice, RSI limits the maximum power of pump-turbines because the dynamic stresses originated in the RSI have become a major root cause of failures. In installed pump-turbines, RSI must be monitored in order to prevent fatigue failures in impeller-runner.

Rotor-stator interaction characteristics can be determined using the analytical model presented by Rodriguez et al. [7]. This model is based on the hypothesis that (1) there is a radial load every time a blade passes in front of a guide vane; (2) the shape of each of these loads is similar; (3) the amplitude of loads depends on which vane is interacting with the blade; and (4) the sequence of loads is given by the combination of number of blades and vanes. With this model the RSI magnitude distribution around the perimeter of pump-turbine can be determined, allowing the identification of conditions of industrial interest, such as an eccentricity or an excessive RSI in a particular vane. The most adequate technique to determine these RSI characteristics is to measure pressure in all the perimeter of the impeller-runner. Unfortunately most pump-turbines are not manufactured considering several drills to locate pressure sensors at these positions. For that reason the RSI is normally analyzed using vibration measurements which in general is affordable and does not require major intervention of the machine. To monitor RSI, the vibration is usually measured in the journal bearing which acts as a filter for vibrations originated in the rotor as it can be noticed in studies about the hydrodynamic bearings response of Qiu and Tieu [10], Jiang and Yu [11], and Pettinato et al. [12]. However, important information of vibration could be lost because bearing response attenuates or amplifies different frequency bands depending on bearing's stiffness and damping. The only way to avoid the effect of the bearing's response in vibration measurements is to measure directly on the shaft which is rotating. To measure on the rotating shaft it is necessary to install vibration sensors capable to work properly rotating on the shaft surface, thus under

a high constant acceleration (due to centripetal acceleration). The electric signal from sensors located on the shaft surface can be obtained by an acquisition system using a slippery ring or telemetry. Nowadays vibration measurements under high constant acceleration and telemetry from rotating shaft to a fixed position are affordable and can be used in the industrial environment. There are a few publications using telemetry in vibration measured rotating with shaft, and the few studies found on hydraulic turbomachinery are focused on the detection of cavitation where the global vibration levels are used as severity indicators. These studies suggest that these measurements are a better indicator of the machine cavitation condition (Farhat et al. [13] and Escaler et al. [14]). The use of telemetry systems to measure vibration on the rotating shaft instead of in the bearings emerges as an opportunity to improve the monitoring of RSI using vibration measurements that are more affordable than pressure measurements in the entire perimeter of the impeller-runner.

The present work aims to monitor RSI using pressure measurements and compare it to the RSI detected using vibrations measured in the bearings and rotating with shaft. The study is carried out in a 100 MW pump-turbine. First, the RSI characteristics are determined from pressure measurements. Then, RSI characteristics are determined from vibrations measured in the bearings and from vibrations measured rotating with shaft. Finally, RSI characteristics determined with both vibration measurements are compared to those obtained analyzing pressure measurements.

## 2. Measurements in Actual Pump-Turbine

The study was carried out in a 100 MW pump-turbine shown schematically in Figure 1. The nominal rotating speed is 600 rpm ( $f = 10$  Hz). The impeller-runner has  $Z_B = 7$  blades, and blade passing frequency is  $Z_B f = 70$  Hz. The diameter of impeller-runner is 2.87 m and the shaft diameter is 0.90 m. The turbine is designed for a net-head of 376 m and a flow-rate of  $32 \text{ m}^3/\text{s}$ . The spiral case has 16 guide vanes and 16 stay vanes (one of the stay vanes corresponds to the cut-water). Measuring positions are shown in Figure 1. Pressure was measured at positions  $P_1$  and  $P_2$  in the low cover and at positions  $P_3$  and  $P_4$  in the channels between guide vanes. Details of pressure measuring positions are shown in Figure 2. Pressure transducers used for these measurements were Wika S-10, with a sensitivity of  $0.2 \text{ mV}/\text{bar}$  ( $\pm 5\%$ ), and a frequency range from 0 to 1000 Hz ( $\pm 10\%$ ). Vibration in bearings was measured using industrial accelerometers at positions  $B_1$  and  $B_2$  in the guide bearing nearest to impeller-runner in radial direction. The accelerometers employed for measurements in bearing were Brüel & Kjær 8325, with a sensitivity of  $98 \text{ mV}/\text{g}$  ( $\pm 5\%$ ), and a frequency range from 1 to 10000 Hz ( $\pm 10\%$ ). Shaft angular position was determined making use of a photoelectric tachometer that detects a reflecting tape located in the shaft. The reflecting tape was located in the same angular position as motor-generator pole no. 1. The photoelectric tachometer was a Brüel & Kjær MM0024 with a frequency range from 3 to 333 Hz. Pressure transducers, accelerometers in bearing, and photoelectric tachometer were conditioned using a 16-channel conditioner Brüel &

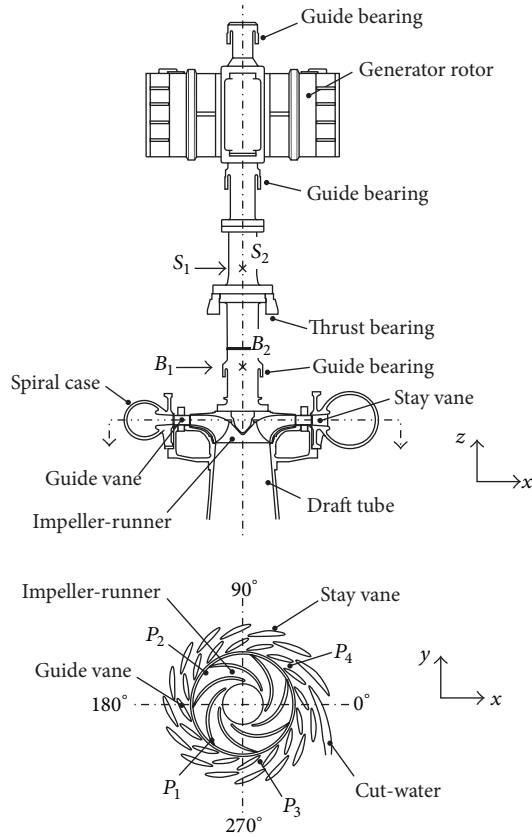


FIGURE 1: Measurements points in 100 MW industrial pump-turbine.

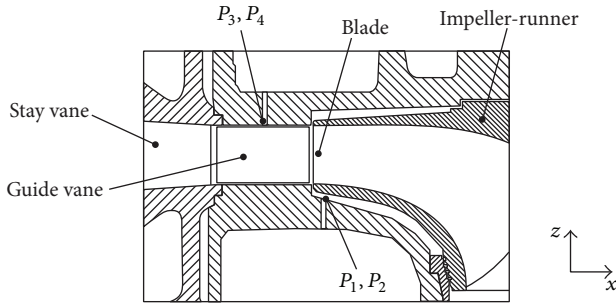


FIGURE 2: Details of position of pressure transducers.

Kjær 2694. Vibration rotating with shaft was measured at positions  $S_1$  and  $S_2$  using industrial accelerometers installed in the shaft surface in radial direction. Accelerometers used to measure vibration rotating with shaft were Brüel & Kjær 4394, with a sensitivity of 9.8 mV/g ( $\pm 5\%$ ), and a frequency range from 1 to 25000 Hz ( $\pm 10\%$ ). Sensors signals from rotating shaft were conditioned and transmitted making use of a KMT MT32 modular telemetry system with a resolution of 12 bits and a frequency range from 0 to 24000 Hz ( $\pm 3$  dB). All measurements were simultaneously recorded using a 16 channel recorder Sony PC216Ax with 16 bits of resolution and a frequency range from 0 to 20000 Hz ( $\pm 10\%$ ). After recording, data was transferred to a computer via a controller board Dspace DS1103. Waveform and spectrum analysis was performed in a computer making use of the software

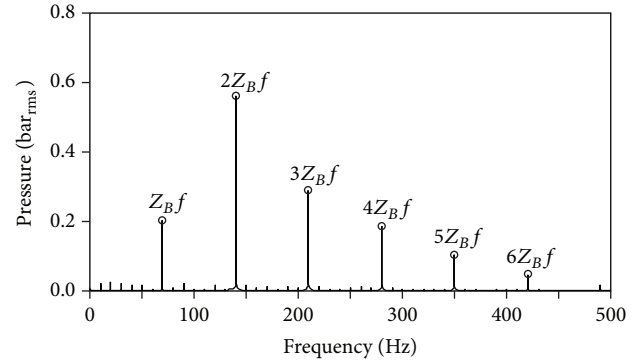


FIGURE 3: Spectrum obtained for  $P_3$  at 100% of guide vane opening.

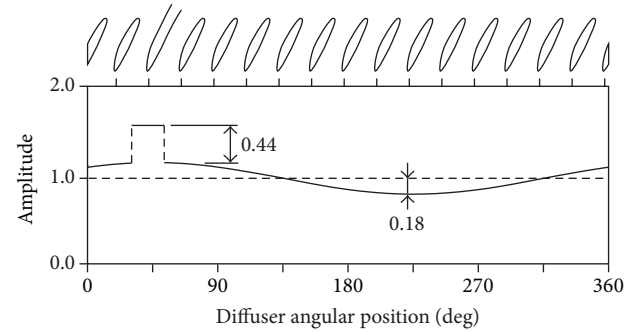


FIGURE 4: RSI distribution determined from pressure measurements.

LabVIEW. To ensure operation under optimal design conditions, all measurements shown in this work were carried out during pump and turbine operation at a 100% guide vane opening. The measurements analysed in this work were performed after the stationary temperature of bearings, lubrication oil, and stator coils was reached. Further details on the measurement technique are available in Mateos-Prieto [15] and Rodriguez [16].

### 3. RSI Characteristics Determined Using Pressure Measurements

Figure 3 shows the spectrum of pressure measured at  $P_3$  when operating at 100% of guide vane opening. Making use of Rodriguez et al. [7]'s model and pressure measurements,  $P_1$ ,  $P_2$ ,  $P_3$ , and  $P_4$ , RSI magnitude around the perimeter of the pump-turbine can be determined taking into account two different distributions of the RSI amplitude. These two distributions are (1) a distributed amplitude and (2) a single rise of amplitude in a particular guide vane. The distributed amplitude is used to account for the fact that there is a sinusoidal variation in amplitude due, for example, to a variable distance between the tip of the blade and the tip of the guide vane, assuming a static eccentricity of the impeller-runner. The single rise in amplitude is used to account for the fact that all the amplitudes are the same except at the single guide vane where the amplitude of interaction is higher. The RSI characteristics determined applying [7] to pressure measurements are shown in Figure 4, where the amplitude of

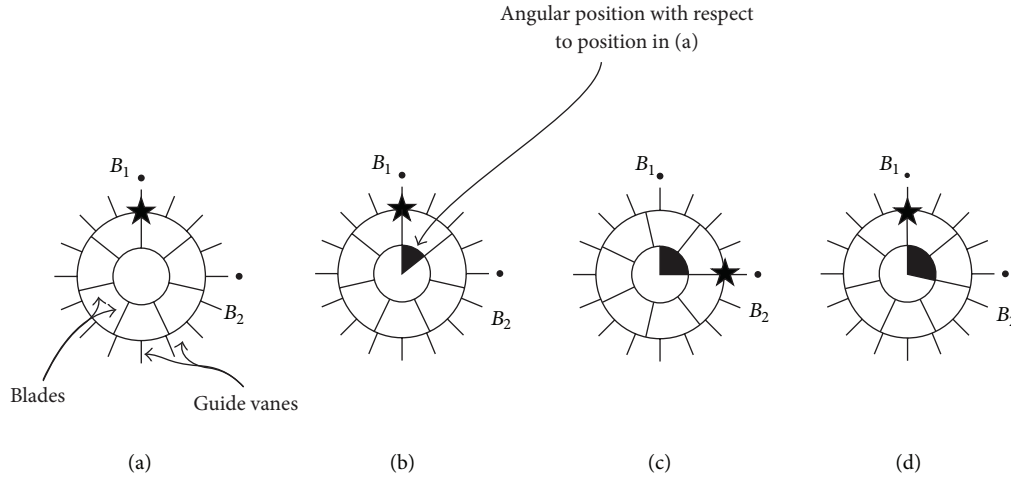


FIGURE 5: Relative positions of the impeller-runner with respect to the guide vanes.

RSI is shown in a normalized way, as the amplitude divided by the expected RSI amplitude found when all interactions have the same amplitude. In order to obtain a waveform of RSI amplitude distribution these two amplitude distributions are added for all blades with the corresponding phase lag. This manual procedure is repeated until a correlation factor reaches a value above 90%. In Figure 4, the corresponding guide vane is shown at the top of the graph.

#### 4. Vibration Measurements and Its Relationship with Rotor-Stator Interaction

The purpose of these vibration measurements is to monitor the RSI characteristics obtained from pressure measurements shown in the previous section. An appropriate vibration monitoring should be able to detect similar characteristics to those shown in Figure 4. In this section, characteristics of RSI are determined using first, vibrations measured in bearings and then vibrations measured rotating with shaft. Waveform and spectrum analysis shown in this section were carried out after performing time synchronous averaging (TSA) to measured vibration. The TSA waveform was obtained considering 20 averages. The spectrum of TSA waveform was computed using 4 averages of 1 second duration (100 revolutions of pump-turbine), obtaining spectrums with frequency resolution of 0.1 Hz.

**4.1. Vibrations Measured in the Guide Bearing.** Vibrations are measured in two perpendicular directions in the guide bearing nearest to impeller-runner, positions labelled  $B_1$  and  $B_2$  in Figure 1. To clarify the relationship between  $B_1$  and  $B_2$ , four graphs are shown in Figures 5 and 6, where  $B_1$  (in solid line) and  $B_2$  (in dashed line) are plotted for a complete turn of the shaft.  $B_1$  is plotted at the reference angular position obtained with the detection of reflective tape ( $0^\circ$ ).  $B_2$  is plotted for four different angular positions at the reference angular position ( $0^\circ$ , Figures 5(a) and 6(a)), and for  $1/Z_B$  (Figures 5(b) and 6(b)),  $1/4$  ( $90^\circ$ , Figures 5(c) and 6(c)), and  $2/Z_B$  (Figures 5(d) and 6(d)) of revolution. At the left and right side

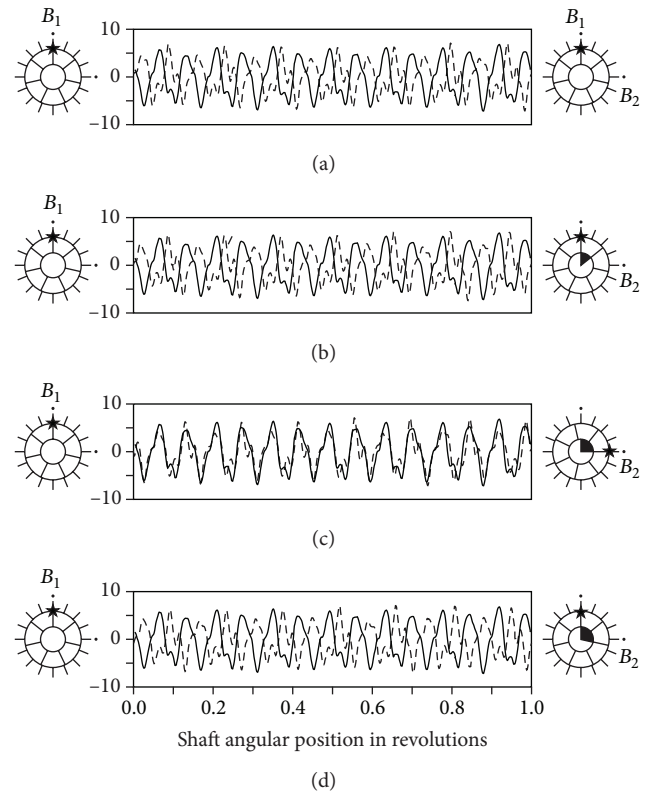


FIGURE 6: Vibration measurements in guide bearing and phase relationship between  $B_1$  and  $B_2$ . Vibration amplitudes in mm/s.

of Figure 5 schematically indicated are the relative positions of the impeller-runner with respect to the guide vanes for plotted  $B_1$  and  $B_2$ , respectively. It can be noticed, that  $B_1$  and  $B_2$  are similar after  $1/4$  of revolution when the same blade passes in front of the position of measurement (Figures 5(c) and 6(c)). At  $1/Z_B$  and  $2/Z_B$  revolutions, the same guide vane interacts with a different rotor blade; however, no similarity can be observed between  $B_1$  and  $B_2$  (Figures 6(b) and 6(d)).

TABLE 1: Amplitudes in spectrums of measurements.

			Relative amplitude			
		$Z_B f$	$2Z_B f$	$3Z_B f$	$4Z_B f$	$5Z_B f$
Pressure	$P_3$	0.35	1.00	0.53	0.35	0.20
Vibration in guide bearing	$B_1$	0.03	1.00	0.02	0.03	0.25
Vibration rotating with shaft	$S_{12}$	0.32	1.00	0.06	0.07	0.05

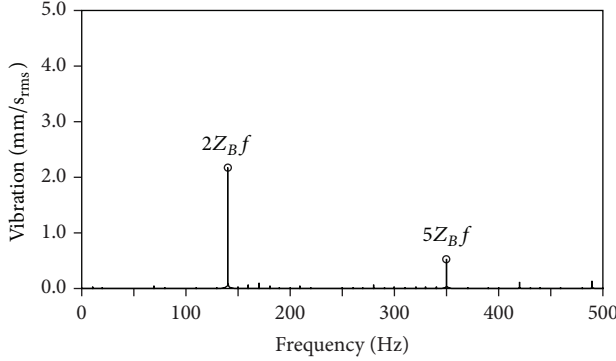
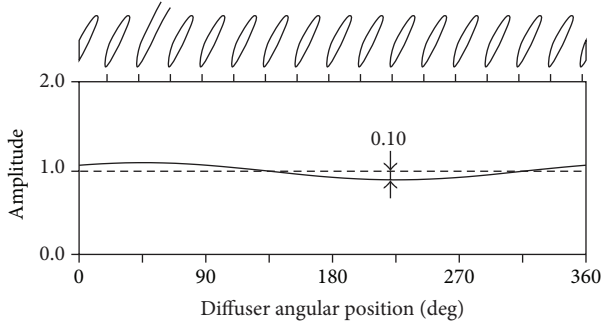
FIGURE 7: Spectrum obtained for  $B_1$  at 100% of guide vane opening.

FIGURE 8: RSI distribution determined from vibration measurements in guide bearing.

This behaviour suggests that the same rotor blade has similar interaction with two different guide vanes.

Figure 7 shows the spectrum of  $B_1$  shown in Figure 6. The distribution of RSI amplitude determined from  $B_1$  and  $B_2$  using the hypotheses of [7] is shown in Figure 8.

**4.2. Vibrations Measured Rotating with the Shaft.** The vibrations measured rotating with shaft are labelled  $S_1$  and  $S_2$  in Figure 1. Four graphs are shown in Figures 9 and 10, where the signal  $S_1$  (in solid line) is plotted at the initial shaft reference position obtained with the detection of reflective tape ( $0^\circ$ ). The signal  $S_2$  (in dashed line) is plotted for different positions of shaft at the reference angular position ( $0^\circ$ , Figures 9(a) and 10(a)); and for  $1/Z_B$  (Figures 9(b) and 10(b));  $1/4$  ( $90^\circ$ , Figures 9(c) and 10(c)); and  $2/Z_B$  (Figures 9(d) and 10(d)) of revolution. At the left and right of each graph the relative position of the impeller-runner with respect to the guide vanes for  $B_1$  and  $B_2$ , respectively, is schematically indicated. It can be noticed that after  $1/Z_B$  of revolution

(Figure 10(b))  $S_1$  and  $S_2$  show a good agreement in the position of peaks and that the signal repeats exactly after  $2/Z_B$  revolutions (Figure 10(d)). At  $1/Z_B$  of revolution  $S_2$  is not in the best position to register the interaction but at  $2/Z_B$  is able to register the interaction in almost maximum amplitude, presenting the same shape as  $S_1$  at the initial shaft reference position (Figure 10(a)). At  $1/4$  of revolution (Figure 10(c)), the same rotor blade interacts but with a different guide vane and no similarity can be observed between  $S_1$  and  $S_2$ . The sensors  $S_1$  and  $S_2$  register the same vibration at the moment a rotor blade interacts with the same guide vane ( $S_1$  at  $0^\circ$  and  $S_2$  after  $2/Z_B$  turns). This behaviour indicates that the interaction of the same guide vane is the same for two different rotor blades.

The spectrum of vibration at  $S_1$  is shown in Figure 11. It can be observed that there are different frequencies to those found in  $B_1$  (Figure 7) and  $P_3$  (Figure 3). This difference is due to the  $\pm f$  modulation in the rotating frame of reference. In order to compare the frequency content of vibration measured rotating with the shaft and in the guide bearing, it was necessary to change frame of reference transforming from the rotating frame to the inertial frame of reference. The expected vibration  $S_{12}$  in the inertial frame of reference was determined from  $S_1$  and  $S_2$  by vectorial addition. Figure 12 shows the spectrum obtained for inertial vibration  $S_{12}$ . The distribution of RSI amplitude determined from  $S_1$  and  $S_2$  using [7] is shown in Figure 13.

## 5. Discussion

From Figures 6 and 7 it can be clearly observed that the vibration measured in bearing is mainly of a sinusoidal form at  $2f_B$  (the amplitude of  $2f_B$  in  $B_1$  and  $B_2$  corresponds to a 75% and a 74% of global RMS value, resp.). It is also observed that  $B_1$  in Figure 7 does not present components at  $Z_B f$ ,  $3Z_B f$ , and  $4Z_B f$  that are of significant amplitude in  $P_3$  (Figure 3).  $S_{12}$  in Figure 12 does have a spectrum similar to  $P_3$  but with lower amplitude of harmonics  $3Z_B f$  to  $6Z_B f$ . Table 1 summarizes the amplitudes in spectrum normalized by the maximum amplitude found in each spectrum that in all measurements corresponds to  $2Z_B f$ . It can be observed that the frequency content of  $P_3$  and  $S_{12}$  is similar for the first two harmonics, while  $B_1$  is similar to  $P_3$  in  $2Z_B f$  and  $5Z_B f$ . These differences in the frequency components are originated in the rotor and guide bearing response for vibrations measured in guide bearings and also due to rotor response in vibrations measured rotating with shaft. It is also observed that the amplitudes obtained for vibration  $S_{12}$  are higher than in  $B_1$ .

The influence of rotor response in previous measurements was determined making use of computed order tracking [17] to track synchronous vibrations with significant



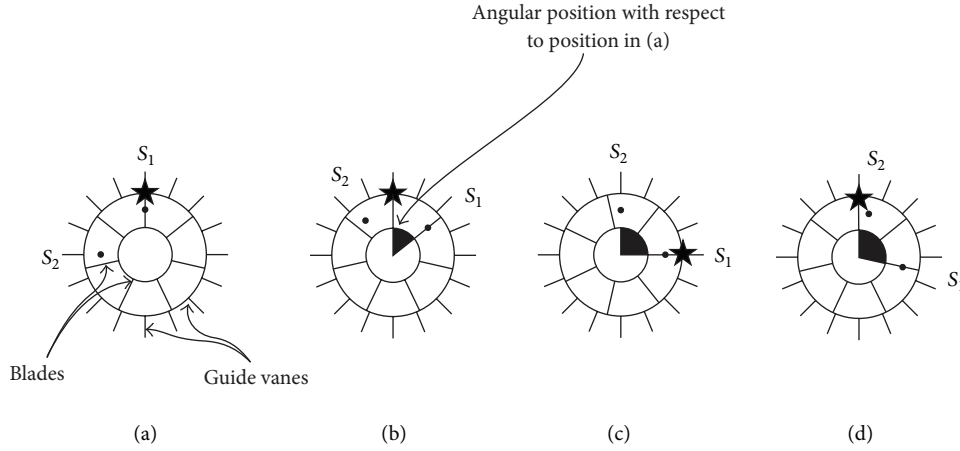


FIGURE 9: Relative positions of the impeller-runner with respect to the guide vanes.

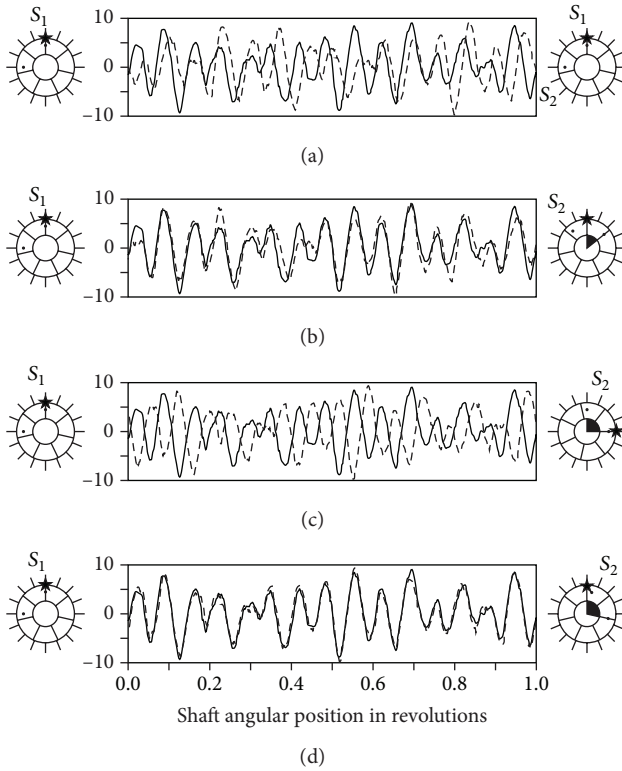


FIGURE 10: Vibration measurements rotating with shaft and phase relationship between  $S_1$  and  $S_2$ . Vibration amplitudes in mm/s.

amplitude (in this case at  $2Z_B f$ ) during a start-up and shut-down test [16]. It was found that the pump-turbine analysed in this work behaves as a rigid rotor; therefore it was concluded that the amplitudes of vibrations of first harmonics of blade passing frequency were not significantly affected by rotor response.

Considering the RSI amplitude distribution in Figures 4, 8, and 13, it can be observed that all measurements allow inferring a distributed amplitude of RSI around the perimeter of impeller-runner presenting the maximum amplitude in

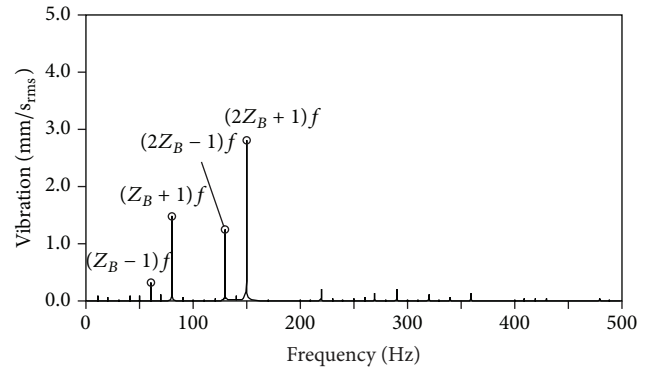


FIGURE 11: Spectrum obtained for  $S_1$  at 100% of guide vane opening.

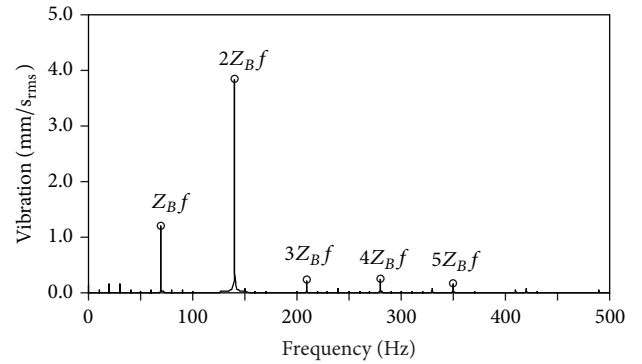


FIGURE 12: Spectrum obtained for  $S_{12}$  at 100% of guide vane opening.

the same position relative to the diffuser, in the angular position of cut-water. This condition is detected mainly by the  $2Z_B f$  component and arises because the impeller-runner centre of rotation does not coincide with the geometric centre of the perimeter defined by the inner edges of the guide vanes. For this reason, the distance between blade and guide vanes varies in the perimeter. Pressure measurements, vibration in guide bearing, and vibration rotating with shaft detect this condition as a  $\pm 18\%$ ,  $\pm 10\%$  and  $\pm 13\%$  of variation,

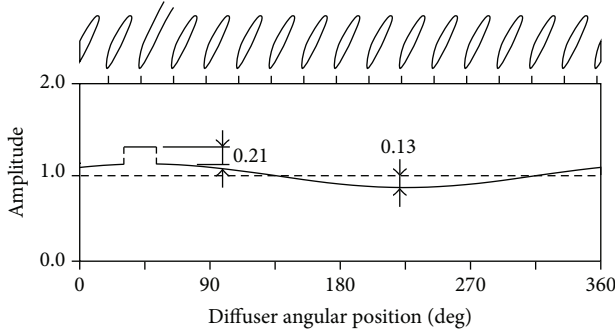


FIGURE 13: RSI distribution determined from vibration measurements rotating with shaft.

TABLE 2: RSI characteristics.

		Eccentricity	Cut-water effect
Pressure	$P_3$	$\pm 18\%$	$+44\%$
Vibration in guide bearing	$B_1$	$\pm 10\%$	$0\%$
Vibration rotating with shaft	$S_{12}$	$\pm 13\%$	$+21\%$

respectively (see Table 2). This percentage variation is relative to the amplitude found for constant amplitude of RSI around the perimeter of impeller-runner.

It can be observed in Figures 4, 8, and 13 that pressure measurements and vibrations measured rotating with shaft allow inferring a single rise in amplitude of RSI with a higher amplitude in the position of cut-water. Vibrations measured in guide bearing do not allow detecting this single rise in amplitude of RSI. Pressure measurements and vibration rotating with shaft do detect this condition at the cut-water as a  $+44\%$  and  $+21\%$  of variation, respectively (see Table 2). This condition is mainly detected by the amplitude and phase relationship between  $Z_B f$ ,  $2Z_B f$ , and  $3Z_B f$  components, information that is lost in vibration measured in guide bearings.

In the case of large hydraulic turbomachinery (usually more than 30 MW), the rotating speed is low (less than 900 rpm) and the shaft is stiff (more than 0.8 m diameter), for these reasons the rotor usually behaves as a rigid rotor (rotating speed is much lower than 0.7 times the first critical velocity). Because of these characteristics, the first rotor critical speed is significantly higher than the first bearing natural frequency; therefore lower harmonics of blade passing frequency in vibrations measured in bearing will be more affected than vibrations measured rotating with shaft. These lower harmonics of blade passing frequency give the main information to determine RSI characteristics. It is important to indicate that in other types of machines with flexible shafts (turbogenerators for example), the difference in RSI detection between measuring in bearings and rotating with shaft will not be as important as in large hydraulic turbomachinery.

## 6. Conclusions

A 100 MW pump-turbine was studied making use of pressure measurements and vibrations measured in guide bearing and rotating with shaft. These measurements were analysed in order to detect RSI characteristics.

Pressure measurements were suitable to monitor and detect RSI characteristics. These RSI characteristics allowed inferring important conditions of pump-turbine such as static eccentricity and an excessive pressure pulsation at a particular position. The RSI characteristics obtained with pressure measurements can also be determined using vibrations measured rotating with shaft. These characteristics cannot be determined using the vibrations measured in guide bearing.

Measurements of vibrations rotating with shaft can be performed in the industrial environment providing data and quality information to help to analyze RSI. The measurements in the shaft provide more comprehensive information about the RSI characteristics, condition that makes it an appropriate technique for the monitoring, and detection of impeller-runner behaviour in pump-turbines.

The difference on the quality of information obtained by vibration measurements in bearing and vibration measurements rotating with shaft is due to the different frequency response of rotor and bearing. This difference is important in the monitoring of RSI in large hydraulic turbomachinery because the lower harmonics of blade passing frequency are affected by the bearing response. It is therefore recommended here that, to detect RSI characteristics in large hydraulic turbomachinery, vibration rotating with shaft should be measured.

## Conflict of Interests

The authors declare that there is no conflict of interests regarding the publication of this paper.

## Acknowledgment

The authors would like to acknowledge the Hydrodyna Eureka Project no. 3246 for financial support.

## References

- [1] N. Arndt, A. J. Acosta, C. E. Brennen, and T. K. Caughey, "Rotor-stator interaction in a diffuser pump," *Journal of Turbomachinery*, vol. 111, no. 3, pp. 213–221, 1989.
- [2] N. Arndt, A. J. Acosta, C. E. Brennen, and T. K. Caughey, "Experimental investigation of rotor-stator interaction in a centrifugal pump with several vaned diffusers," *Journal of Turbomachinery*, vol. 112, no. 1, pp. 98–108, 1990.
- [3] R. S. Miskovich and C. E. Brennen, "Some unsteady fluid forces on pump impellers," *Journal of Fluids Engineering*, vol. 114, no. 4, pp. 632–637, 1992.
- [4] S. Guo and H. Okamoto, "An experimental study on the fluid forces induced by rotor-stator interaction in a centrifugal pump," *International Journal of Rotating Machinery*, vol. 9, no. 2, pp. 135–144, 2003.

- [5] R. Spence and J. Amaral-Teixeira, "A CFD parametric study of geometrical variations on the pressure pulsations and performance characteristics of a centrifugal pump," *Computers and Fluids*, vol. 38, no. 6, pp. 1243–1257, 2009.
- [6] A. Ozturk, K. Aydin, B. Sahin, and A. Pinarbasi, "Effect of impeller-diffuser radial gap ratio in a centrifugal pump," *Journal of Scientific and Industrial Research*, vol. 68, no. 3, pp. 203–213, 2009.
- [7] C. G. Rodriguez, E. Egusquiza, and I. F. Santos, "Frequencies in the vibration induced by the rotor stator interaction in a centrifugal pump turbine," *Journal of Fluids Engineering*, vol. 129, no. 11, pp. 1428–1435, 2007.
- [8] A. Coutu, M. D. Roy, C. Monette, and B. Nennemann, "Experience with rotor-stator interactions in high head Francis runner," in *Proceedings of the 24th IAHR Symposium on Hydraulic Machinery and Systems*, Foz do Iguassu, Brazil, October 2008.
- [9] E. Egusquiza, C. Valero, X. Huang, E. Jou, A. Guardo, and C. Rodriguez, "Failure investigation of a large pump-turbine runner," *Engineering Failure Analysis*, vol. 23, pp. 27–34, 2012.
- [10] Z. L. Qiu and A. K. Tieu, "Identification of sixteen force coefficients of two journal bearings from impulse responses," *Wear*, vol. 212, no. 2, pp. 206–212, 1997.
- [11] P. L. Jiang and L. Yu, "Dynamics of a rotor-bearing system equipped with a hydrodynamic thrust bearing," *Journal of Sound and Vibration*, vol. 227, no. 4, pp. 833–872, 1999.
- [12] B. Pettinato, R. D. Flack, and L. E. Barrett, "Test results for a highly preloaded three-lobe journal bearing—effect of load orientation on static and dynamic characteristics," *Lubrication Engineering*, vol. 57, no. 9, pp. 23–30, 2001.
- [13] M. Farhat, F. Avellan, and U. Seidel, "Pressure fluctuation measurements in hydro turbine models," in *Proceedings of the 9th International Symposium on Transport Phenomena and Dynamics of Rotating Machinery*, Honolulu, Hawaii, USA, February 2002.
- [14] X. Escaler, E. Egusquiza, M. Farhat, and F. Avellan, "Cavitation erosion prediction in hydro turbines from onboard vibrations," in *Proceedings of the 22nd IAHR Symposium on Hydraulic Machinery and Systems*, Stockholm, Sweden, July 2004.
- [15] B. Mateos-Prieto, *Experimental contribution to rotor stator interaction in pump-turbine prototypes [Doctoral Thesis]*, Technical University of Catalonia, 2005.
- [16] C. G. Rodriguez, *Feasibility of on board measurements for predictive maintenance in large Hydraulic turbomachinery [Doctoral Thesis]*, Technical University of Catalonia, 2006.
- [17] P. N. Saavedra and C. G. Rodriguez, "Accurate assessment of computed order tracking," *Shock and Vibration*, vol. 13, no. 1, pp. 13–32, 2006.



